IOP Publishing Superconductor Science and Technology
Supercond. Sci. Technol. 31 (2018) 105012 (6pp) https://doi.org/10.1088/1361-6668/aadbfd

Vortex dynamics driven by AC magnetic field in YBCO thin films with complex pinning structures

I Ivan, A M Ionescu, V Sandu, A Crisan and L Miu

National Institute of Materials Physics, 77125 Bucharest-Magurele, Romania

E-mail: ion.ivan@infim.ro

Received 28 February 2018, revised 6 August 2018
Accepted for publication 21 August 2018
Published 10 September 2018

Abstract

We investigated the AC magnetic response of a $YBa_2Cu_3O_7$ film with embedded $BaZrO_3$ nanorods and Y_2O_3 nanoparticles at a static magnetic field H_{dc} lower than the matching field H_{Φ}. We proposed a practical formula for the determination of the induced current J during AC susceptibility measurements, which allows us to directly obtain the pinning potential U_c from the characteristics of electric field E versus J. We show that the dynamic critical current J_d induced at the depinning frequency f_d can be experimentally obtained by measuring $m'(T)$ and $m''(T)$ at different frequencies and amplitudes. It was found that the value of f_d obtained by extrapolation of J to J_d in the PHz domain is much higher than the frequency reported for ordinary $YBa_2Cu_3O_7$ thin films as determined by microwave impedance measurements.AC susceptibility, vortex dynamics, pinning energy, depinning frequency, dynamic critical current, microwave impedance measurements

(Some figures may appear in colour only in the online journal)

1. Introduction

To enhance the critical current density in superconductors, the response of vortices to linear and oscillatory Lorentz forces is widely investigated either by the relaxation of the irreversible magnetization in constant magnetic field H_{dc} (DC relaxation) [1] or by AC susceptibility $\chi = \chi' - i\chi''$ (or, equivalently, AC magnetic moment $m = m' - im''$) measurements using an external periodic magnetic field $h = h_{ac}\cos(2\pi ft)$ at frequencies f, spanning roughly, from 1 Hz to several kHz, and amplitudes h_{ac} between 0.1 Oe and tens of Oe.

In this situation the response of the vortex system is rather complex [2] but extremely useful for the study of the flux pinning properties. Specifically, at small enough amplitude h_{ac} of the AC-field, the slow deformation of the vortex lattice at the surface propagates into the interior and vortices oscillate inside the pinning potentials. In this so-called Campbell regime, with a h_{ac}-independent screening [3], it is possible to determine the average curvature of the pinning potential [4] and to investigate the field and temperature dependence of the critical current density J [5]. At higher h_{ac}, vortices overcome the pinning well and the flux line system enters into a more dissipative regime with h_{ac}-dependent magnetic response. In this case, the effective vortex activation energy U_{eff} has a logarithmic dependence on the induced current density J of the form:

$$U_{eff} = U_c \ln\left(\frac{J_d}{J}\right), \tag{1}$$

where U_c is the characteristic pinning energy and J_d is the dynamic critical current density, i.e., the induced current at the depinning frequency f_d of the AC magnetic field, above which vortices move freely in a highly dissipative process with a real resistivity [6, 7]. Indeed, if the motion of the flux line under an alternating current $J = J_0 e^{i2\pi ft}$ is treated as a damped harmonic oscillator with a restoring force proportional to the curvature of the pinning potential well and a damping proportional to the vortex viscosity η [7], the vortex motion generates a complex resistivity which depends on frequency as [8, 9]:

$$\rho = \frac{B\phi_0}{\eta c^2}\frac{1}{1 + if_d/f}, \tag{2}$$

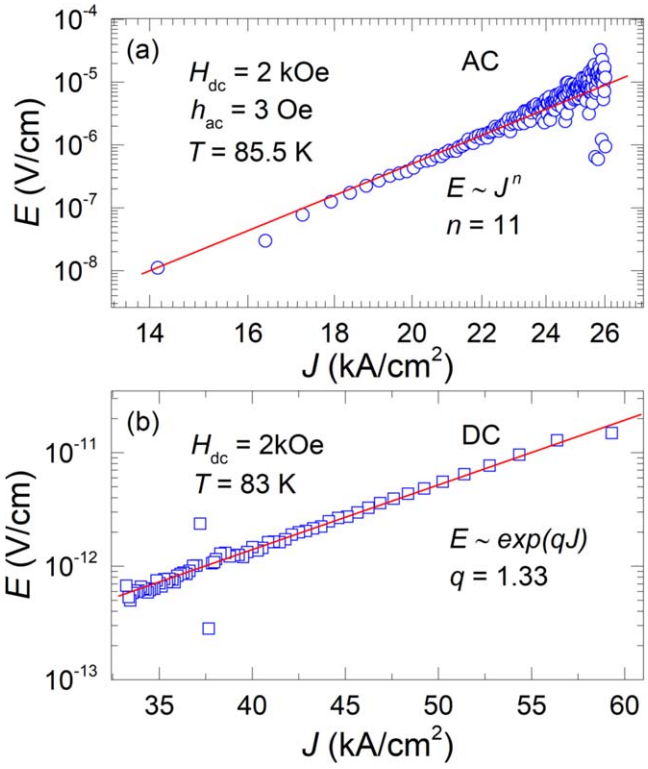

Figure 1. (a) *E–J* characteristics at short time scale, as obtained from $m'(t = 1/f)$ at $T = 85.5$ K, $h_a = 3$ Oe, $H_{dc} = 2$ kOe, in a log–log plot. (b) *E–J* dependence, as extracted from DC magnetization relaxation data at $T = 83$ K and $H_{dc} = 2$ kOe, shown in a semi-log plot.

where B is the magnetic induction, ϕ_0 the vortex quantum and $\eta \approx \frac{H_{c2}\phi_0}{\rho_n c^2}$ (H_{c2} is the upper critical magnetic field, and ρ_n is the sample resistivity in the normal state). According to equation (2) for a frequency $f \gg f_d$ the flux motion shows a crossover from the pinning regime with complex resistivity to a free flux flow where the resistivity $\rho = \frac{B\phi_0}{\eta c^2}$ is real. As was experimentally proved in [9], the depinning frequency f_d, is proportional to the pinning constant (Labusch parameter) α_c:

$$f_d \propto \frac{\alpha_c \rho_n}{H_{c2}\sqrt{B\phi_0}}. \tag{3}$$

In a previous work [10] we have investigated the AC magnetic response of the same $YBa_2Cu_3O_7$ (YBCO) film and we have found high U_{eff} values even the data were collected in close proximity to the DC irreversibility line (IL).

In this work we focus on J_d determination for h_{ac} between 0.5 and 6 Oe in static magnetic field $H_{dc} = 2$ and 10 kOe and, by extrapolation, we show that J attains the order of magnitude of $J_d \sim 10^5$ A cm^{-2} at a frequency $f_d = 10^{11}$ Hz. Also, we proposed a practical formula for J induced during AC susceptibility measurements. This allows us to construct the $E(J)$ dependence in AC regime by measuring m' at frequencies between 10 and 10 000 Hz and to compare the results with $E(J)$ curve obtained from standard DC magnetization relaxation data at appropriate temperatures.

2. Experimental details

The $YBa_2Cu_3O_{7-x}$ composite film (2.2×2.2 mm^2, 0.4 μm thickness) with embedded $BaZrO_3$ (BZ) nanorods and Y_2O_3 (YO) nanoparticles was prepared on $SrTiO_3$/MgO substrate by pulsed-laser deposition from a YBCO + $BaZrO_3$ composite target with a thin Y_2O_3 sector stuck on the top. The critical temperature (corresponding to the onset of the diamagnetic signal in a DC magnetic field of 10 Oe) was $T_c = 88.6$ K. The value of the matching field H_Φ, i.e, the field where the vortex density and that of columnar pins are equal, was 20 kOe as determined from transmission electron microscopy. The preparation conditions and microstructure details are presented elsewhere [11].

AC susceptibility measurements have been performed using a Physical Property Measurement System (Quantum Design) after the sample was cooled down from temperatures $T > T_c$ to 50 K in the DC field H_{dc} perpendicularly oriented to the film surface. The AC-field amplitude was between 0.5 and 6 Oe at frequencies in the range 11–5555 Hz. The measurements were performed in static DC magnetic fields of 2 and 10 kOe. For comparison, zero-field cooling DC magnetic relaxation data were registered with an MPMS magnetometer (Quantum Design) with H_{dc} in the same field-sample geometry.

3. Results and discussion

To obtain information about the flux dynamics and pinning potential we used an AC susceptibility technique which will be described below. It is known that the in-phase component of the AC magnetic moment m' is proportional to the screening current density J, whereas the out-of-phase component m'' is a measure of dissipation and has a maximum at the peak temperature T_p where the flux front reaches the sample centre [10]. For a thin disk in a perpendicular field, the critical current density J_c, at T_p where the sample is fully penetrated, is given by [12]

$$J_c(T_p) = 1.03\frac{h_{ac}}{d}, \tag{4}$$

where d is the thickness of the disk. Alternatively, for $T > T_p$, we can use another approach to calculate J_c within the framework of the critical state model, considering only the real part χ' of the ac susceptibility [12]:

$$\chi' = \chi_0(1.33 \cdot x^{-\frac{3}{2}} - 0.634 \cdot x^{-\frac{5}{2}}),\ x \gg 1, \tag{5}$$

where R is the disk radius, $\chi_0 = 8R/3\pi d$, and $x = 2h_{ac}/J_c d$. For practical units, considering only the first term, the above equation can be rewritten as

$$J_c = 159 \cdot \frac{h_{ac}^{1/3}}{d}\left(\frac{9.4}{\chi_0}|M'|\right)^{2/3}, \tag{6}$$

with J_c in A m^{-2}, h_{ac} in Oe, the volume magnetization M' in emu cm^{-3} and d in metres.

In order to obtain the *E–J* characteristics, we used the approach from [13] and estimated the electric field E at the

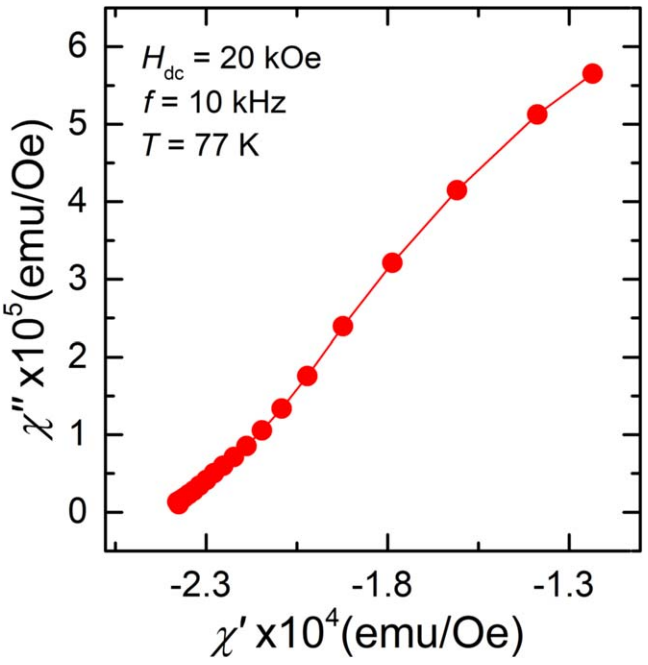

Figure 2. Cole–Cole plot of the AC susceptibility as measured at f= 10 kHz, H_{dc} = 20 kOe and T = 77 K., for h_{ac} in the range 0–16 Oe.

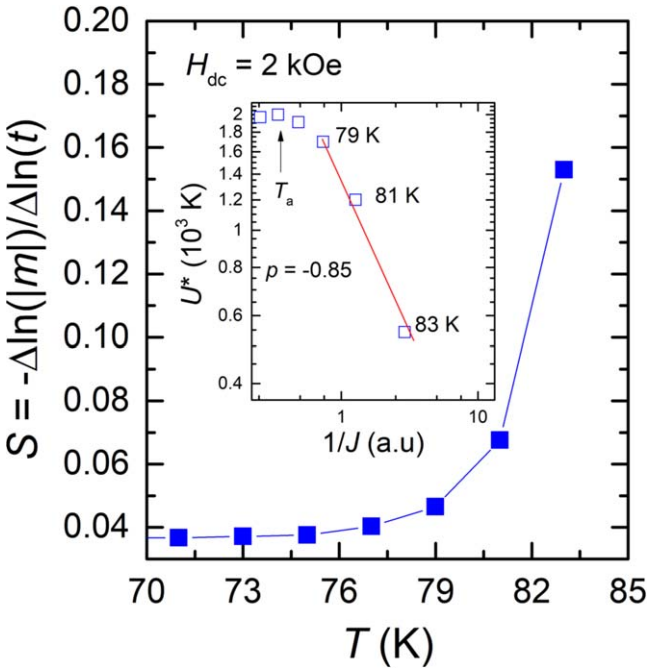

Figure 3. Temperature T dependence of the relaxation rate of the DC magnetization S at a constant field of 2 kOe. Inset: normalized vortex activation energy $U^* = -T/S$ versus $1/J$ in log–log scale (J was obtained from the first point in $m(t)$ curve using the Bean model).

sample edge ($x = a/2$) for a square cross section of size a perpendicular to the H_{dc} as:

$$E = \frac{2\pi}{c}(1 - D)a\frac{dM}{dt}, \tag{7}$$

where M is the volume magnetization and D is the demagnetization factor with $1 - D = 10^{-4}$ precisely determined from the initial slope of the DC magnetization curves obtained in increasing H_{dc} with a step of 1 Oe.

Thereupon, by measuring the frequency dependence (f range spans from 1 Hz to 10 kHz) of the in-phase AC magnetic moment m', we transformed $m'(f)$ in $E(J)$ using equation (6) and equation (7). The E–J characteristic obtained by this procedure is shown in figure 1(a) for H_{dc} = 2 kOe, h_{ac} = 3 Oe.

It is important to mention that in order to the make a correct interpretation of the AC data, we first had to rule out the presence of flux avalanches which are usually observed at a short time scale [1]. With this aim, we measured $\chi''(h_{ac})$ versus $\chi'(h_{ac})$ at 77 K and H_{dc} = 20 kOe, for h_{ac} in the range 0–16 Oe, and the results were used to obtain the Cole–Cole plot from figure 2. The smoothness of this plot confirms the critical state regime according to [14].

The $E(J)$ variation is easily understood as being determined by the J dependence of the effective creep barrier U_{eff} [13], by considering that $E = vB/c$ (where v is the vortex velocity and B the magnetic induction) and with the well known Arrhenius law $f = f_0\exp(-U/T)$ (f_0 is the characteristic attempt frequency and we took $k_B = 1$), we obtain:

$$E \propto \exp\left(-\frac{U_{eff}(J)}{T}\right). \tag{8}$$

The linearity of the log(E) versus log(J) plot from figure 1(a), which is present in the AC investigations, is in agreement with equation (1). In this case, the slope $n = U_c/T$ provides the characteristic pinning energy U_c = 940.5 K. As it will be shown below, this value is close to the value obtained from the slope of $J(t)$ dependence in log–log scale. For comparison, in the case of the classic vortex creep which occurs during the relaxation of the DC magnetic moment m, the effective vortex activation energy obeys a different law [1, 10]:

$$U_{eff}(J) = \frac{U_c}{p}\left[\left(\frac{J_{c0}}{J}\right)^{|p|} - 1\right], \tag{9}$$

where J_{c0} is the creep free critical current and p is the creep exponent. In this case, E versus J dependence can be obtained using equation (8) for E and the well known Bean formula for J [15].

As we can see in figure 1(b) the $E(J)$ characteristic shows linearity in semi-log plot which is consistent with the plastic creep regime for which $p = -1$; hence, equation (8) can be read as:

$$E \propto \exp(qJ), \tag{10}$$

where $q = U_c/TJ_{c0} = 1.33$.

In order to confirm the value of p, we made $m(t)$ measurements in DC magnetic field, more exactly, we measured the magnetization relaxation rate $S = \Delta\ln(|m|)/\Delta\ln(t)$ versus temperature T as is shown figure 3. As might be seen for

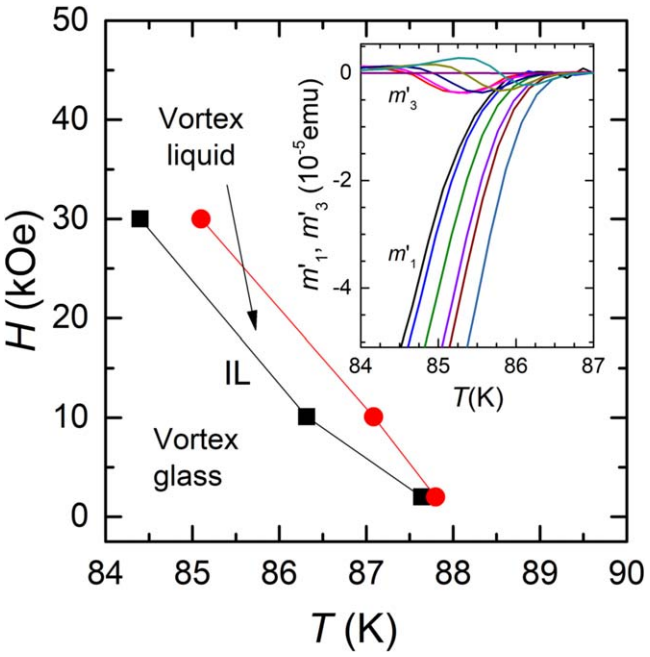

Figure 4. Phase diagram for the $YBa_2Cu_3O_{7-x} + BaZrO_3 + Y_2O_3$ thin film up to 30 kOe. The full squares mark the irreversibility line (IL), as obtained from the onset of third harmonics $m_3'(T)$ extrapolated at $f = 0$ for $h_{ac} = 0.5$ Oe. $H_{c2}(T)$, as deduced from the onset of $m_1'(T)$, is plotted with full circles. Inset: temperature dependence of $m_1'(T)$ and $m_3'(T)$ at $h_a = 0.5$ Oe and $H_{dc} = 10$ kOe for different frequencies f from left to right: 11; 21.5; 111; 555; 1111; and 5555 Hz.

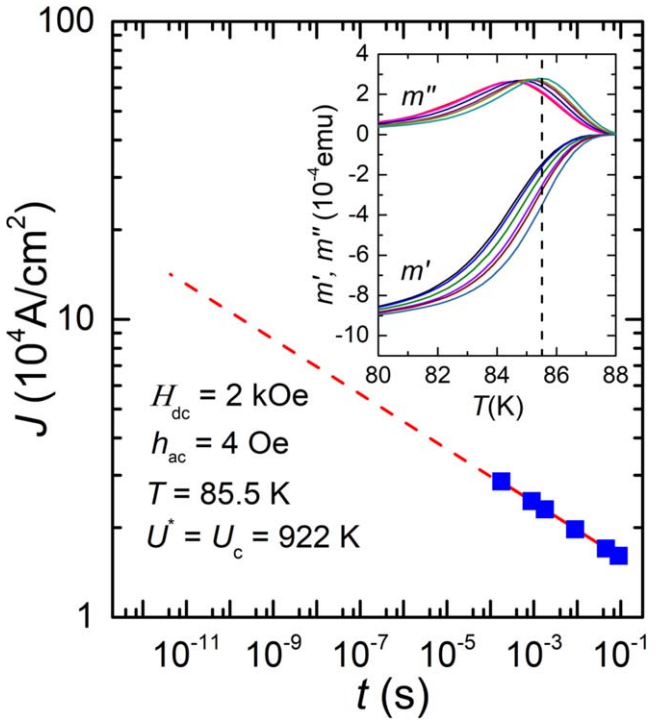

Figure 5. The induced current density J versus $t = 1/f$ ($H_{dc} = 2$ kOe, $h_{ac} = 4$ Oe) at $T = 85.5$ K. The dashed line is the extrapolation of J within the range of $J_d \sim 10^5$ A cm^{-2}. Inset: the temperature T dependence of the in-phase m' and out-of-phase m'' components of the AC magnetic moment (after the sample had been cooled from above T_c to 75 K) with $h_a = 4$ Oe for different frequencies f from left to right: 11; 21.5; 111; 555; 1111; and 5555 Hz.

$T > T_a = 75$ K, S increases fast due to the strong thermal fluctuations which smear out the pinning potential [16]. The fast increase of S is consistent with the fast decrease of the normalized vortex activation energy U^* [1]:

$$U^* = -\frac{T}{S} = -T\frac{\Delta \ln(t)}{\Delta \ln(|m|)} \tag{11}$$

and a plastic creep process similar to nonuniform single vortex creep dominates de flux dynamics [17, 18]. In this scenario, it is known that for a magnetic relaxation curve at given H_{dc} and T, $U^*(J) = U_c(J_{c0}/J)^p$ [10], so the creep exponent p can be obtained from the linear fit of U^* versus $1/J$ in log–log scale which in our case provides $p \sim -1$ (see the inset to figure 3).

For a better understanding of our data, specifically, the (H, T)-range relative to the IL (the line in H–T diagram that separates the vortex liquid region from the region where the vortices are pinned), we proceeded to build the IL from the plot of the onset of third harmonics $m_3'(T, H_{dc})$ extrapolated at $f = 0$ for $h_{ac} = 0.5$ Oe. Figure 4 shows the phase diagram obtained in this way to which we have added the upper critical field as deduced in the same way from the onset of first harmonic of the AC susceptibility $m_1'(T, H_{dc})$.

It is well known that by crossing IL the vortex system melts and the pinning energy should be within the order of magnitude of the thermal energy. According to figure 4, our AC data were taken close to IL, a fact which would make the high value of U_c as obtained from AC investigations surprising. In our opinion, this effect is caused by a less effective smearing of U_c due to a high flux velocity in a non-diffusive vortex dynamics during the AC cycle. Indeed, for $H_{dc} = 2$ kOe, the electric field values in the AC regime are several orders of magnitude higher than in the DC regime and that leads to an average vortex velocity $v \propto E/B$ of 0.3 cm s^{-1} comparative to only 1 nm s^{-1} as obtained from DC magnetization relaxation data. In these circumstances, the local force that a vortex experiences in AC regime can be described by a higher effective viscous drag coefficient $\eta \propto \exp(U_{eff}/T)$ which exceeds the Barden–Stephen coefficient η_0 by many orders of magnitude [19].

Regarding AC susceptibility measurements, we can estimate the values of J_d induced at the depinning frequency f_d of the magnetic field, from the equation (1) as

$$J_d = J \exp\left(\frac{U_{eff}}{Uc}\right). \tag{12}$$

Therefore, measuring $m'(T)$ for different f at fixed h_{ac} and H_{dc} and transforming m' in J for every frequency at a constant T (see the dashed line in the inset of figure 5), we directly obtain $U^* = U_c$ by linearly fitting the time ($t = 1/f$) dependence of J in log–log scale (see figure 5). To assure that the sample is fully penetrated for all frequencies and the equation (6) can be applied, we chose a temperature where the imaginary part of the AC magnetization $m''(T)$ measured at the highest frequency $f_{max} = 5555$ Hz, reaches a peak,

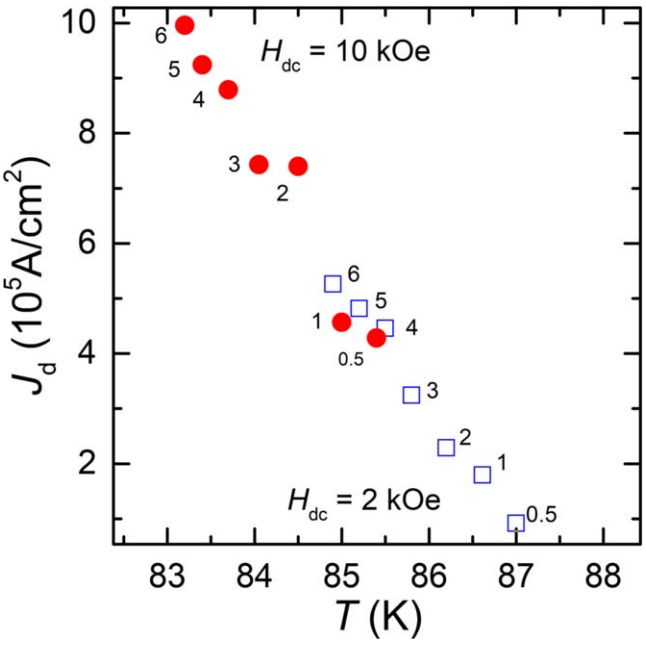

Figure 6. Experimental determination of J_d at $T = T_p$ (5555 Hz) for $H_{dc} = 2$ kOe (open squares) and 10 kOe (filled circles) at various h_{ac} (marked with text labels near every point on the graph).

i.e., at $T = T_p(f_{max} = 5555\,\text{Hz})$. For example, at $h_a = 4$ Oe we have $T_p(f_{max}) = 85.5$ K.

In this case, the linearity of the log(J) versus log(t) plot, as shown in the main panel of figure 5 indicates the validity of the equation (1), thus $U^* = U_c = -T\frac{\Delta \ln(t)}{\Delta \ln(J)} = 922$ K which is very close to the value obtained from $E(J)$ curve from figure 1(a).

Close values were previously reported in [20] and also from microwave impedance measurements but the definition of the pinning/activation energy is not always similar. For example, in YBCO-ZB films, Pompeo *et al* reported a value $U_{min} \approx 313$ K at $T = 83$ K, and a measuring frequency of 47.7 GHz [21] but U_{min} is the lowest height of the potential barrier.

Finally, following the manner described in [10], with $U_{eff}(J, 0\,\text{K})$ obtained from ln(f) versus $1/T_p$ plot, the value of the effective pinning energy at $T = T_p(f_{max})$ can be estimated using the relation $U_{eff}(J, T) = U_{eff}(J, 0\,\text{K})(1 - T/T_c)$.

Thus, for fixed h_a and H_{dc}, having U_c, U_{eff} and $J(T_p(f_{max}))$ extracted with equation (4) we can obtain J_d according to equation (12) as represented in figure 6, for h_{ac} in the range 0.5–6 Oe in a static magnetic field of 2 and 10 kOe.

It is very important to notice that the extrapolation to the high-f region in the log(J) versus log(t) plot from the main panel of figure 5 indicates that the J would attain the order of magnitude of J_d at $f = f_d = 10^{11}$ Hz if we take $J_d \sim 10^5\,\text{A cm}^{-2}$, i.e., the depinning frequency reported in other papers for YBCO [22, 23 and references therein]. However, in our case the extremely strong pinning structures (BZ nanorods and YO nanoparticles) lead to higher depinning current densities (e.g., $J_d \cong 4 \times 10^5\,\text{A cm}^{-2}$ for $H_{dc} = 2$ kOe, $h_{ac} = 4$ Oe) which would correspond to a depinning frequency of order of PHz. This is not surprising because for high values of U_c, the depinning frequency obtained by extrapolation increases fast with J_d as $f_d \propto J_d^k$ [10], where k is superunitary (for example in figure 5, $k \sim 11$).

4. Conclusions

In summary we propose a practical formula for the determination of the induced current during AC susceptibility measurements at $T > T_p$ and the characteristic pining energy obtained from both $E(J)$ characteristics and $J(t = 1/f)$ dependence at short time scale was $U_c(85.5\,\text{K}) \approx 900$ K. It was found that, for $H_{dc} = 2$ kOe, the flux velocity during AC measurements is $v = 0.3\,\text{cm s}^{-1}$ and only $1\,\text{nm s}^{-1}$ in DC relaxation measurements. Thus, the thermal smearing of the potential walls is reduced in AC experiments (as described in [24]) and the obtained U_c is always higher than U_c determined from DC magnetic measurements. Also, the dynamic critical current J_d induced for AC driven forces at depinning frequencies was experimentally obtained by measuring m' and m'' as a function of T, for different f, h_{ac} and H_{dc}. The depinning frequency f_d extracted by the extrapolation of J to the order of magnitude of $J_d \sim 10^5\,\text{A cm}^{-2}$ is in agreement with the values obtained from microwave impedance measurements.

Acknowledgments

Financial support from Romanian Ministry of Research and Innovation through POC (European Regional Development Fund, Operational Fund Competitiveness) Project P-37_697 number 28/01.09.2016 and Core Programme PN18-110201 is gratefully acknowledged.

ORCID iDs

I Ivan https://orcid.org/0000-0001-9203-9444
A Crisan https://orcid.org/0000-0002-0662-0177
L Miu https://orcid.org/0000-0003-0007-6331

References

[1] Ivan I, Miu D, Popa S, Jakob G and Miu L 2011 *Supercond. Sci. Technol.* **24** 095005
[2] Miu L, Mele P, Ivan I, Ionescu A M and Miu D 2015 *J. Supercond. Novel Magn.* **28** 361–5
[3] Pasquini G, Civale L, Lanza H and Nieva G 1999 *Phys. Rev.* B **59** 9627
[4] Silhanek A V, Raedts S, Lange M and Moshchalkov V V 2003 *Phys. Rev.* B **67** 064502
[5] Raedts S, Silhanek A V, Moshchalkov V V, Moonens J and Leunissen L H A 2006 *Phys. Rev.* B **73** 174514
[6] Poole C Jr, Farach H, Creswick R and Prozorov R 2014 *Superconductivity* (Amsterdam: Elsevier) (https://doi.org/10.1016/C2012-0-07073-1)
[7] Gittleman J I and Rosenblum B 1966 *Phys. Rev. Lett.* **16** 734

[8] Suhl H 1965 *Phys. Rev. Lett.* **14** 226
[9] Matsuda Y, Ong N P, Yan Y F, Harris J M and Peterson J B 1994 *Phys. Rev.* B **49** 4380
[10] Ivan I, Ionescu A M, Miu D, Mele P and Miu L 2016 *Supercond. Sci. Technol.* **29** 095013
[11] Mele P, Matsumoto K, Horide T, Ichinose A, Mukaida M, Yoshida Y and Kita R 2008 *Supercond. Sci. Technol.* **21** 015019
[12] Clem J R and Sanchez A 1994 *Phys. Rev.* B **50** 9355
[13] Brandt E H 1995 *Phys. Rev.* B **52** 15442
[14] Motta M, Colauto F, ZadorosnyR, Johansen T H, Dinner R B, Blamire M G, Ataklti G W, Moshchalkov V V, Silhanek A V and Ortiz W A 2011 *Phys. Rev.* B **84** 214529
[15] Bean C P 1964 *Rev. Mod. Phys.* **36** 31–6
[16] Blatter G, Feigel'man M V, Geshkenbein V B, Larkin A I and Vinokur V M 1994 *Rev. Mod. Phys.* **66** 1125 and references therein
[17] Miu L *et al* 2010 *J. Phys.: Conf. Ser.* **234** 012026
[18] Miu L, Mele P, Ivan I, Ionescu A M, Crisan A, Badica P and Miu D 2014 Magnetization, relaxation in superconducting $YBa_2Cu_3O_7$ films with embedded nanorods and nanoparticles *Size Effects in Nanostructures* (*Springer Series in Materials Science* vol 205) ed V Kuncser and L Miu (Berlin: Springer) ch 9 p 293
[19] Vanevic M, Radovic Z and Kogan V G 2013 *Phys. Rev.* B **87** 144501
[20] Crisan A, Awang Kechik M M, Mikheenko P, Dang V S, Sarkar A, Abell J S, Paturi P and Huhtinen H 2009 *Supercond. Sci. Technol.* **22** 045014
[21] Pompeo N, Rogai R, Augieri A, Galluzzi V, Celentano G and Silva E 2009 *J. Appl. Phys.* **105** 013927
[22] Golosovsky G, Tsindlekht M and Davidov D 1996 *Supercond. Sci. Technol.* **9** 1–15
[23] Zhou X-Q *et al* 2013 *Phys. Rev.* B **87** 184512
[24] Miu L, Ivan I, Ionescu A M and Miu D 2016 *AIP Advances* **6** 065027